Scientific Research Publishing

Journal of Geoscience and Environment Protection, 2025, 13(12), 260-278
https://www.scirp.org/journal/gep
ISSN Online: 2327-4344
ISSN Print: 2327-4336

Trend and Frequency Analysis of Long-Term Maximum Daily Rainfall in Benin

Ezéchiel Obada[1,2*], Freddy Zinsè Hounnondaho[1,3], Halissou Yarou[1,2], Orou Moctar Ganni Mampo[2,4], Adéchina Eric Alamou[1,2]

[1]Laboratoire de Géoscience, de l'Environnement et Applications (LaGEA)/Ecole Nationale Supérieure des Travaux Publics (ENSTP)/Université Nationale des Sciences, Technologies, Ingénierie et Mathématiques (UNSTIM), Abomey, Bénin
[2]Laboratoire d'Hydrologie Appliquée (LHA)/Institut National de l'Eau (INE)/Université d'Abomey-Calavi (UAC), Cotonou, Benin
[3]Ecole Doctorale des Sciences, Technologies, Ingénierie et Mathématiques (ED-STIM)/Université Nationale des Sciences, Technologies, Ingénierie et Mathématiques (UNSTIM), Abomey, Bénin
[4]Graduate Research Programme on Climate Change and Water Resources (GRP CCWR), West African Science Service Centre on Climate Change and Adapted Land Use (WASCAL), Université d'Abomey Calavi, Cotonou, Benin
Email: *obada.ezechiel@unstim.bj

How to cite this paper: Obada, E., Hounnondaho, F. Z., Yarou, H., Mampo, O. M. G., & Alamou, A. E. (2025). Trend and Frequency Analysis of Long-Term Maximum Daily Rainfall in Benin. *Journal of Geoscience and Environment Protection, 13,* 260-278.
https://doi.org/10.4236/gep.2025.1312014

Received: September 11, 2025
Accepted: December 7, 2025
Published: December 10, 2025

Abstract

The objective of this study is to assess the trends and predict the maximum daily rainfall using Benin century rainfall gauges. The Pettitt, Buishand, and entropy breakpoint detection tests were employed to identify stationarity breaks, while the Mann-Kendall trend test was used to assess trends. Stationary and non-stationary Generalized Extreme Value (GEV) distributions are used to conduct the frequency analysis. From 1921-2020, a significant increasing trend is detected at Abomey and Adjohoun stations with a slope of 0.17 and 0.16 mm/year, respectively, while a significant decreasing trend is found at Allada, Cotonou, Natitingou, and Savè stations with a slope of −0.24, −0.20, −0.13, and −0.21, respectively. Other stations exhibit a non-significant trend over the entire period of study. However, some of these stations exhibit a significant increasing or decreasing trend before or after the breakpoint. The frequency analysis shows that the stationary GEV distribution provides a good fit for rainfall time series without a significant trend, while the non-stationary GEV model better fits the series exhibiting significant trends. The results also show that many stations have recorded the precipitation of a 150 - 200-year return period, indicating the level of exposure of the region to extreme events.

Keywords

Trend, Stationarity Breakpoint, Frequency Analysis, Maximum Daily Rainfall

1. Introduction

The 1950s were characterized by unprecedented disruptions in the global climate system (Yang et al., 2022). Climate change is undeniably one of the most significant challenges facing humanity today. Climate change is not a localized phenomenon, but a global issue that affects both human societies and ecosystems (Kuniyal et al., 2021). Climate change is primarily driven by human activities, such as the burning of fossil fuels and biomass, as well as large-scale deforestation (Ampofo et al., 2023; Kumar et al., 2023). The IPCC report (IPCC, 2021) highlights that human activities are responsible for the 1.1˚C increase in global temperature since the pre-industrial era. These long-term changes in the Earth's climate are leading to increased variability in the distribution, frequency, and intensity of meteorological events (El Kasri et al., 2021). Changes in patterns of extreme events are one of the most significant manifestations of climate change (IPCC, 2007). Among these extreme events, extreme rainfall constitutes a major hazard.

In order to define strategies for adapting to climate change, it is important to study the behaviour of precipitation in general and extreme rainfall in particular. Many studies were carried out to assess the impacts of climate change on extreme rainfall at global, regional, and local scales. Donat et al. (2016) indicated that extreme precipitation events increased in recent decades at the global scale. In northern China (Jing-Jin-Ji district), Mei et al. (2018) showed that the extreme precipitation indices have downward trends. Gao et al. (2017) pointed out that extreme precipitation indices have significant increasing trends, except for maximum consecutive dry days, showing an increasing probability of flood-induced catastrophes over the Monsoon region in China. Over southeastern South America, observed precipitation showed an increasing trend in the annual maximum of daily precipitation over the period from 1955-2005 (Wu & Polvani, 2017). In West Africa, trend analysis reveals both increasing and decreasing patterns in extreme rainfall. Obada et al. (2021) identified increasing and decreasing trends in maximum one-day and five-day precipitation patterns over the period 1961-2016 in Benin. Kougbeagbede et al. (2024) indicate a marginal increase in maximum daily rainfall at Cotonou. Kpanou et al. (2021) found an increasing trend in extreme rainfall events throughout the southern part of Ivory Coast, Togo, and Benin. However, most studies on extreme rainfall over West Africa were based on relatively short meteorological data, generally over 1950-2020. To study the effects of climate change, it is important to assess prevailing trends in climate conditions using long-term meteorological data. Long-term trend assessment can help to develop strategies for adaptation and mitigation, minimizing the potential negative impacts of climate change. The objective of this study is to assess the trends and predict the maximum daily rainfall using Benin century rainfall gauges. To achieve this, the Pettitt, Buishand, and entropy breakpoint detection tests were employed to identify stationarity breaks, while the Mann-Kendall trend test was used to assess trends. Stationary and non-stationary Generalized Extreme Value (GEV) distributions are used to conduct the frequency analysis. This study is of particular significance for Benin, as rainfall is a crucial component of the region's economy. In fact, agriculture is the backbone of most economies in sub-Saharan Africa, contributing up to 14% of the gross domestic product in these countries (OECD/FAO). Agriculture is the primary economic sector in Benin, contributing 35% to the country's gross domestic product, 75% of export earnings, 15% of national income, and providing approximately 70% of employment (PAM, 2014). It also plays a crucial role in ensuring food security. In 2020, agriculture employed 52% of the workforce in West Africa (World Bank, 2011), while in Benin, this figure was around 29%. Agriculture is largely rain-fed, making it highly vulnerable to climate change. Changes in rainfall distribution can directly or indirectly impact agricultural production, human livelihoods, water resource management, and the structure and function of ecosystems (Kumar et al., 2023). For instance, increasing temperatures and changing rainfall patterns in the 1970s and 1980s significantly affected agricultural production, resulting in decreased crop and livestock yields and disrupting food distribution (IPCC, 2007), leading to famine in West Africa. The findings of this study will be valuable for developing more effective climate change adaptation strategies.

2. Study Area and Methods

2.1. Study Area

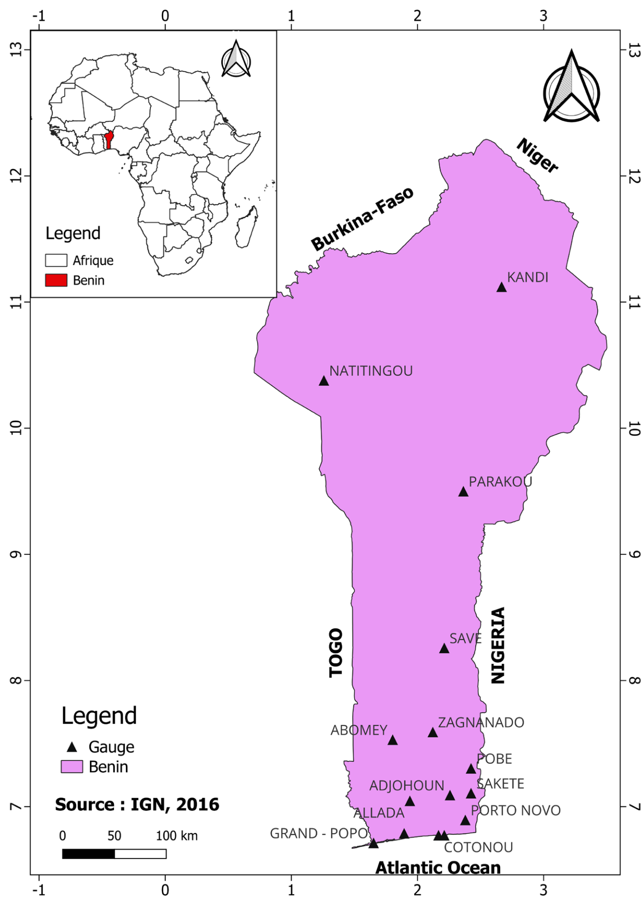

Figure 1. Study area and rain gauge locations.

Benin is a West African country with an elongated shape, oriented perpendicularly to the coast of the Gulf of Guinea (Obada et al., 2017). It covers an area of 112,622 km^2 and is bordered to the north by Niger and Burkina Faso, to the east by Nigeria, to the west by Togo, and to the south by the Atlantic Ocean (**Figure 1**). The country is influenced by the West African monsoon and has a continental tropical climate. In the northern part, there is a single rainy season (April to October) and a dry season (November to March), while the southern part experiences two rainy seasons (April to July and September to November) and two dry seasons (December to March and August). Annual precipitation ranges from 700 mm to 1400 mm, and the annual mean temperature varies between 23˚C and 32˚C (Obada et al., 2017; Obada et al., 2021).

2.2. Data and Methods

- Data

In this study, the observed rainfall data were provided by the National Agency of Meteorology of Benin (Météo Bénin). The stations were selected following a rigorous quality control procedure, which involved detecting missing values, outliers, and transcription errors for manually operated stations. Only stations with less than 5% missing data during the rainy seasons from 1922 to 2020 were included in the analysis.

- Mann-Kendall Test

The Mann-Kendall test is a non-parametric test commonly used to detect monotonic trends in series of meteorological data, hydrological data, environmental data, etc. (Mann, 1945; Kendall, 1975; Bera, 2017). The main advantages of the Mann-Kendall test are the low sensitivity in homogeneous time series (Jaagus, 2006) and the non-requirement of normally distributed time series (Tabari & Talaee, 2011) since the test is non-parametric. The null hypothesis (H0) shows no trend in the series, and data, which come from an independent population, are identically distributed. The alternative hypothesis (H1) indicates that the data follow a monotonic trend (upward or downward trend). It is calculated following these equations.

$$S \equiv \sum_{i=1}^{n-1} \sum_{j=i+1}^{n} sign\left(x_j - x_i\right) \tag{1}$$

where $\boldsymbol{x_i}$ and $\boldsymbol{x_j}$ are the annual values in years i and j, $\boldsymbol{j > i}$ and

$$sign\left(x_j - x_i\right) \equiv \begin{cases} 1 \quad if\ x_j - x_i > 0 \\ 0 \quad if\ x_j - x_i = 0 \\ -1\ if\ x_j - x_i < 0 \end{cases} \tag{2}$$

The mean of S is E [S] = 0 and the variance of S is computed by

$$\boldsymbol{VAR}\left(\boldsymbol{S}\right) = \frac{1}{18}\left[\boldsymbol{n}\left(\boldsymbol{n}-1\right)\left(2\boldsymbol{n}+5\right) - \sum_{p=1}^{q} \boldsymbol{t}_p\left(\boldsymbol{t}_p - 1\right)\left(2\boldsymbol{t}_p + 5\right)\right] \tag{3}$$

where n is a number of data points, q is the number of tied groups and t_p is the number of data values in the pth group.

Normal approximation (Z statistic) is generally used when the sample size is more than 10. Z statistic is given by Equation (4).

$$\boldsymbol{Z}=\begin{cases}\dfrac{\boldsymbol{S}-1}{\sqrt{\boldsymbol{VAR}(\boldsymbol{S})}} & \boldsymbol{if}\ \boldsymbol{S}>0\\ 0 & \boldsymbol{if}\ \boldsymbol{S}=0\\ \dfrac{\boldsymbol{S}+1}{\sqrt{\boldsymbol{VAR}(\boldsymbol{S})}} & \boldsymbol{if}\ \boldsymbol{S}<0\end{cases}\tag{4}$$

A positive Z value denotes increasing trend, while a negative Z value indicates decreasing trend. At α level of significance, (H0) is rejected if the absolute value of Z is greater than $\boldsymbol{Z}_{1-\alpha/2}$, where $\boldsymbol{Z}_{1-\alpha/2}$ is obtained from the standard cumulative distribution tables (Bera, 2017; Tabari & Talaee, 2011)

- Theil-Sen Slope

The magnitude of a trend was also assessed by using the Theil-Sen estimator (Sen, 1968). This slope is a robust estimation of the magnitude of a trend (Bera, 2017; Tabari & Talaee, 2011) and it is calculate as following:

$$\boldsymbol{b}=\boldsymbol{median}\left(\frac{\boldsymbol{x}_j-\boldsymbol{x}_i}{\boldsymbol{t}_j-\boldsymbol{t}_i}\right)\tag{5}$$

where $\boldsymbol{x}_i$ and $\boldsymbol{x}_j$ are the variable values at times t_i and t_j, respectively.

- Pettitt Test

The Pettitt test (Pettitt, 1979) is based on the Mann-Whitney test but incorporates modifications. It is a rank-order test, making it non-parametric and distribution-free. The test is considered robust, with its power performance being superior to that of the Wilcoxon test and its adapted version for studying stationarity.

$$\boldsymbol{U}(\boldsymbol{t})=\sum_{\boldsymbol{i}=1}^{\boldsymbol{t}}\sum_{\boldsymbol{j}=\boldsymbol{t}+1}^{\boldsymbol{n}}\boldsymbol{signe}(\boldsymbol{x}_i-\boldsymbol{x}_j)\tag{6}$$

$$T=\max\left\{\left|U(t)\right|,t=1\ldots n\right\}\tag{7}$$

$$K=\max\left\{\left|\frac{U(t)}{\sqrt{nt-t^2}}\right|,t=1\ldots n\right\}\tag{8}$$

The sign function is defined as follows

$$\begin{cases}\forall x>0, signe(\boldsymbol{x})=1\\ x=0, signe(\boldsymbol{x})=0\\ \forall x<0, signe(\boldsymbol{x})=-1\end{cases}\tag{9}$$

Calculation of the probability p, the probability of exceeding the k value taken by the test statistic T on the observed series.

$$\boldsymbol{p}=\boldsymbol{P}(\boldsymbol{T}\geq\boldsymbol{k})=2\boldsymbol{exp}\left(\frac{-6\boldsymbol{k}^2}{\boldsymbol{T}^3+\boldsymbol{T}^2}\right)\tag{10}$$

$\boldsymbol{If}\ \boldsymbol{p}<\boldsymbol{\alpha}$ then the null hypothesis is rejected

For the K statistic, <<p>> can be calculated using the bootstrap method.

➢ Buishand Test

The Buishand statistic (Buishand, 1982) is derived from an original formulation given by Gardner (1969). The Gardner statistic used for a two-tailed mean-break test at an unknown time is written as:

$$G = \sum_{k=1}^{N-1} p_k \left\{ S_k / \sigma_X \right\}^2 \tag{11}$$

with $S_k = \sum_{i=1}^{k} \left(X_i - \bar{X} \right)$.

p_k denotes the a priori probability that the rupture will occur after the kth observation. This formulation assumes that the variance σ^2 is known. If not, it can be replaced by the sample variance D_X^2 et si p_k is chosen to be uniform, we finally obtain the U statistic defined by:

$$U = \frac{\sum_{k=1}^{N-1} p_k \left\{ S_k / D_X \right\}^2}{N \left(N+1 \right)} \tag{12}$$

with $D_X^2 = \frac{\sum_{i=1}^{k} \left(X_i - \bar{X} \right)^2}{N}$. Critical values of the U statistic have already been given by Buishand (1982) using a Monte Carlo procedure. Better estimates were published later (Buishand, 1984).

➢ Cross-Entropy

The Entropy-Crossing method is one of the significant advancements in stochastic optimization and simulation in recent years (Morio et al., 2011). Proposed by Rubinstein and Kroese (2004), this method can be effectively applied to analyze time series of flow data to identify potential breakpoints (Equation 13).

$$H = \sum_{i=1}^{N} p_{x_i} \log \left(q_{x_i} \right) \tag{13}$$

where p is the true probability distribution of the series and q is the predicted probability.

Each test relies on different statistical assumptions and exhibits specific sensitivities to various types of changes in the data distribution. The Pettitt test is particularly effective for detecting abrupt shifts in the mean, whereas the Buishand test focuses on gradual changes and variations in variance. The Cross-Entropy test, on the other hand, adopts an information-theoretic approach that captures more subtle and complex changes in the distribution beyond simple mean variations. The combined use of these tests therefore allows for cross-validation of the detected change points, reducing the risk of false detections (Wijngaard et al., 2003; Kang & Yusof, 2010; Khaliq & Ouarda, 2006).

➢ Frequency Analysis

The frequency analysis was carried out using the Generalized Extreme Value (GEV) distribution, following the methodologies of Coles (2001). Based on key assumptions regarding the nature of rainfall variability, both stationary and non-stationary forms of the GEV distribution were employed. Specifically, a stationary GEV model and three non-stationary GEV models were considered to capture potential temporal changes in GEV distribution parameters. The stationary GEV (GEV0) distribution is defined by Equation 14.

$$F(x,\mu,\sigma,\xi) = exp\left\{-\left[1+\xi\left(\frac{x-\mu}{\sigma}\right)\right]^{-1/\xi}\right\} \tag{14}$$

were μ, σ et ξ are respectively the location, scale and shape parameters of GEV distribution. In theory μ, $\xi \in \mathcal{R}$ but in practice, the shape parameter $\xi \in]-0.5;0.5[$ (Martins and Stedinger, 2001). The parameters must satisfy the following conditions: $\sigma > 0$ and $1+\xi\left(\frac{x-\mu}{\sigma}\right) > 0$. The expression for the quantile x_p of the probability of not exceeding precipitation p is (Chikobvu & Chifurira, 2015):

$$x_p = \begin{cases} \mu - \frac{\sigma}{\xi}\left[1-\{-\log(1-p)\}^{-\xi}\right] & for\,\xi \neq 0 \\ \xi - \sigma log\{-\log(1-p)\} & for\,\xi = 0 \end{cases} \tag{15}$$

To take in account the impacts of climate change on extreme precipitations, the stationary GEV distribution is extended to a non-stationary form by allowing its parameters to vary with covariates. These covariates may include time or physical variables such as local or global temperature (Hajani, 2022; Jayaweera et al., 2024). In this study, time is used as the covariate to capture temporal trends. Three assumptions are considered in formulating the non-stationary GEV distributions:

- GEV1: the location parameter varies with time, the scale parameter is a function of the position parameter and the shape parameter is a constant. (Prosdocimi & Kjeldsen, 2021) ($\mu(t) = \mu_1(t) + \mu_0$, σ and $\xi = constant$).
- GEV2: the location and scale parameters vary, while the shape parameter is a constant. ($\mu(t) = \mu_1(t) + \mu_0$, $log\sigma(t) = \sigma_1(t) + \sigma_0$ and $\xi = constant$) (Jayaweera et al., 2025).
- GEV3: all parameters vary ($\mu(t) = \mu_1(t) + \mu_0$, $log\sigma(t) = \sigma_1(t) + \sigma_0$ et $\xi(t) = \xi_1(t) + \xi_0$) (Jayaweera et al., 2025).

To identify the most appropriate model for frequency analysis, the Akaike Information Criterion (AIC) and the Bayesian Information Criterion (BIC) were employed as model selection criteria. The model with the lowest AIC and BIC values was selected as the most appropriate. This approach ensures an optimal balance between model goodness-of-fit and parsimony, thereby reducing the risk of overfitting (Coles, 2001; Katz et al., 2002). When AIC and BIC led to different model selections, priority was given to BIC due to its stronger penalty for model complexity, which is particularly suitable for relatively small sample sizes (Claeskens & Hjort, 2008).

3. Results and Discussion

3.1. Rainfall Trends and Breakpoints

Overall, the analysis of maximum daily rainfall from 1921 to 2020 reveals spatially heterogeneous trends in maximum daily rainfall. In the northern region, a general decreasing trend in rainfall is observed, with these trends typically being weak and largely non-significant. The central region exhibits contrasting patterns, showing an increase in rainfall at Parakou and decreasing trends at Savè. In the southern and coastal stations, a general upward trend is observed, with a few exceptions (e.g., Allada and Cotonou) showing significant downward trends. Breakpoints generally occur around the 1940s, 1960s, and 1980s, which is consistent with the major climatic patterns observed in West Africa (Table 1).

Table 1 shows trends and breakpoints in maximum daily rainfall. At Natitingou, a non-significant downward trend was observed from 1921 to 2020, while a non-significant upward trend was detected at Kandi station. The Pettitt and Buishand stationarity break tests identified breakpoints in 1977 and 1971, respectively, at Natitingou station, while both tests located the break in 1961 and 1962 at Kandi station. The entropy method detected the break in 1980 at Kandi, while at Natitingou, it was detected in 1978. The Mann-Kendall test reveals downward trends before and after the breakpoints at Kandi, and upward trends at Natitingou. Of these trends, only the upward trend in the period after the Pettitt break (1978-2020) at Natitingou is statistically significant at the 95% threshold, with a slope of 5 mm/year.

At the central stations, an upward trend of 1.04 mm/decade, significant at the 90% threshold, was detected over the period 1921-2020 at Parakou. In contrast, at Savè, a downward trend of 2 mm/decade, significant at the 95% threshold, was observed over the same period. The Pettitt and Buishand stationarity break tests indicated breakpoints in 1936 at Savè station and in 1974 at Parakou station, respectively. The entropy method identified the breakpoint in 1982 for Savè station and in 1939 for the Parakou station. The Mann-Kendall test revealed statistically insignificant upward or downward trends for all series obtained after the breakpoints were detected at both stations.

In the south, over the period 1921-2020, increasing trends in maximum daily rainfall were observed at Zagnanado, Adjohoun, and Abomey stations, while decreasing trends were observed at Sakété and Allada stations. Among these trends, only the stations of Adjohoun, Abomey, and Allada are statistically significant, with slopes of 1.7, 1.69, and −2.4 mm/decade, respectively. No trends were detected at Pobè. The Pettitt and Buishand stationarity break tests detected breakpoints in 1986 at Pobè, 1988 at Abomey, 1958 at Adjohoun, and 1968 at Allada. At Sakété and Zagnanado stations, the two tests identified breakpoints at different dates: the Pettitt test detected breaks in 1991 and 1941, respectively, at Zagnanado and Sakété stations, while the Buishand test identified breaks in 1999 at Zagnanado and 1968 at Sakété. The Mann-Kendall test, applied to the sub-periods obtained after the Pettitt and Buishand stationarity break tests, revealed a statistically significant downward trend at the 95% threshold at the Pobè station over the period 1987 to 2020, with a slope of −2.1 mm/year.

Segmentation of the Sakété series using the Pettitt test shows an upward trend in maximum daily rainfall that is significant at the 90% threshold, with a slope of 2.8 mm/year over the period 1921-1941. However, all other sub-periods show non-significant trends across all stations. The entropy method locates breaks in 1949 at Zagnanado, 1987 at Abomey, 1939 at Pobè, and 1958 at Sakété, Adjohoun, and Allada rainfall stations. For the series segments obtained using entropy, a significant trend was detected only at the Allada station at the 95% threshold, over the period 1958-2020, with a slope of −5.4 mm/decade.

Table 1. Trends and breakpoints in maximum daily rainfall.

Station	Trend for all series	Buishand			PETTITT			Cross Entropy		
		Break point Year	Trend Slope Before	Trend Slope After	Break point Year	Trend Slope Before	Trend Slope After	Break point Year	Trend Slope Before	Trend Slope After
Abomey	0.17*	1987	0.04	0.14	1987	0.04	0.14	1987	0.09	0.43
Adjohoun	0.16*	1957	−0.39	−0.06	1957	−0.39	−0.06	1958	−0.39	−0.06
Allada	−0.24*	1968	0.14	−0.37	1968	0.14	−0.37	1958	0.09	−0.54*
Bopa	0.02	1969	0.63	0.8*	1969	0.63	0.8*	1959	−0.04	0.00
Cotonou	−0.20*	1976	0.09	0.34	1976	0.09	0.34	1977	0.09	0.34
Grand Popo	0.03	1937	0.45	0.25	1966	−0.39	−0.48	1958	−0.04	0.15
Kandi	0.05	1962	−0.28	0	1961	−0.32	0	1980	0.08	0.5
Natitingou	−0.13*	1970	0.13	0.17	1978	0.04	0.54*	1978	0.04	0.45
Ouidah	0.09	1959	−0.5	−0.06	1959	−0.5	−0.06	1941	0.07	0.36
Parakou	0.10	1974	−0.19	−0.13	1974	−0.19	−0.13	1939	−1.17	0.16
Pobè	0.00	1986	−0.17	−2.1*	1986	−0.17	−2.1*	1939	1.76	−0.06
Porto Novo	−0.04	1969	0.62	0.33	1969	0.62	0.33	1948	0.51	−0.35
Sakété	−0.02	1967	0.21	0.31	1941	2.83	0.1	1957	0.00	−0.04
Savè	−0.21*	1936	5.04	−0.02	1937	2.42	0	1982	−0.83*	0.54
Zagnannado	0.06	1999	−0.02	−0.53	1990	−0.05	0.27	1949	−0.18	−0.01

*indicates a significant trend.

At rainfall stations along the coast over the period 1921-2020, an upward trend was observed at Grand Popo, Ouidah, and Bopa, while a downward trend was seen at Cotonou and Porto Novo. Of these trends, only the downward trend at Cotonou is statistically significant at the 95% level, with a slope of −2 mm/decade. The Pettitt and Buishand stationarity break tests detected breakpoints in 1959 at Ouidah, 1976 at Cotonou, 1969 at Porto-Novo, and 1969 at Bopa. A discrepancy was observed for Grand Popo, where the Pettitt test identified a break in 1968, while the Buishand test placed the break in 1936. The cross-entropy method found breaks in 1958 at Grand Popo, 1941 at Ouidah, 1978 at Cotonou, 1948 at Porto-Novo, and 1959 at Bopa stations. The Mann-Kendall test, applied to the sub-periods before and after the stationarity breaks identified by Pettitt and Buishand, reveals a non-significant upward trend at the Cotonou and Porto Novo stations, compared to a non-significant downward trend at Ouidah. At the Bopa station, an upward trend of 8 mm/decade, statistically significant at the 95% threshold, was found for the period 1970 to 2020. Additionally, an upward trend of 6.3 mm/decade, significant at the 90% threshold, was detected for the period 1921 to 1969. At Grand Popo, the sub-periods identified by the Pettitt test show a non-significant downward trend, while for the Buishand test, both sub-periods show a non-significant upward trend.

3.2. Selected Models for Frequency Analysis

Table 2. Summary of best-fit distribution and parameters for maximum daily rainfall.

Station	Model	μ (SE)	$\sigma(SE)$	$\xi(SE)$
Abomey	GEV1	$\mu_0 = 66.87(2.02)$ $\mu_1 = 0.15(0.05)$	$\sigma_0 = 17.24(1.57)$	$\xi_0 = 0.141(0.09)$
Adjohoun	GEV1	$\mu_0 = 70.41(2.32)$ $\mu_1 = 0.18(0.07)$	$\sigma_0 = 20.78(1.67)$	$\xi_0 = 0.035(0.06)$
Allada	GEV2	$\mu_0 = 62.73(2.14)$ $\mu_1 = -0.38(0.06)$	$\sigma_0 = 18.31(1.67)$ $\sigma_1 = -0.15(0.06)$	$\xi_0 = 0.088(0.07)$
Bopa	GEV0	$\mu_0 = 72.27(2.40)$	$\sigma_0 = 21.14(1.76)$	$\xi_0 = 0.043(0.07)$
Cotonou	GEV2	$\mu_0 = 90.56(3.50)$ $\mu_1 = -0.46(0.11)$	$\sigma_0 = 30.32(2.57)$ $\sigma_1 = -0.23(0.09)$	$\xi_0 = -0.063(0.07)$
Grand Popo	GEV0	$\mu_0 = 76.04(3.02)$	$\sigma_0 = 26.06(2.29)$	$\xi_0 = 0.111(0.07)$
Kandi	GEV0	$\mu_0 = 61.26(1.84)$	$\sigma_0 = 16.12(1.36)$	$\xi_0 = 0.046(0.07)$
Natitingou	GEV2	$\mu_0 = 62.18(1.83)$ $\mu_1 = -0.10(0.05)$	$\sigma_0 = 15.28(1.42)$ $\sigma_1 = 0.09(0.04)$	$\xi_0 = 0.034(0.09)$
Ouidah	GEV0	$\mu_0 = 85.32(3.32)$	$\sigma_0 = 27.95(2.48)$	$\xi_0 = 0.021(0.09)$
Parakou	GEV0	$\mu_0 = 71.56(2.09)$	$\sigma_0 = 18.18(1.56)$	$\xi_0 = 0.063(0.07)$
Pobè	GEV0	$\mu_0 = 71.82(2.22)$	$\sigma_0 = 19.42(1.63)$	$\xi_0 = 0.013(0.07)$
Porto Novo	GEV0	$\mu_0 = 89.43(2.85)$	$\sigma_0 = 24.75(2.06)$	$\xi_0 = -0.023(0.07)$
Sakété	GEV1	$\mu_0 = 70.41(2.16)$	$\sigma_0 = 19.02(1.55)$	$\xi_0 = 0.071(0.07)$
Savè	GEV2	$\mu_0 = 73.67(2.90)$ $\mu_1 = -0.14(0.07)$	$\sigma_0 = 23.29(2.24)$ $\sigma_1 = -0.35(0.06)$	$\xi_0 = 0.081(0.09)$
Zagnannado	GEV0	$\mu_0 = 66.61(1.77)$ $\mu_1 = 0.09(0.04)$	$\sigma_0 = 14.96(1.37)$	$\xi_0 = 0.121(0.09)$

Table 2 presents the GEV models that best fit the maximum daily rainfall data based on the AIC and BIC selection criteria, along with the corresponding model parameters. Among the tested models, the stationary GEV (GEV0) provided the best fit for the Bopa, Grand-Popo, Kandi, Ouidah, Parakou, Pobè, Sakété, and Porto-Novo stations (8 of 15 stations). The GEV1 model, incorporating a time-varying location parameter, was more suitable for the Abomey, Adjohoun, and Zagnanado stations, while the GEV2 model best fitted data from Allada, Cotonou, Natitingou, and Savè. **Figure 2** illustrates the observed and predicted probability density and quantile plots for Grand-Popo, Adjohoun, Cotonou, and Savè, where

GEV0, GEV1, GEV1, and GEV2 were selected, respectively. The probability density plots demonstrate that the models accurately capture the variability of maximum daily rainfall. At Grand-Popo, the GEV0 distribution provides an almost perfect fit, as reflected in the close match between observed and predicted densities. Similar accuracy was observed at other stations where GEV0 was selected. The GEV1 and GEV2 models also performed well, although quantile-quantile (Q-Q) plots revealed some deviations in the upper tail, particularly in representing extreme outliers. At Grand-Popo, the GEV0 model slightly underestimates the final observation, while at stations such as Savè and Natitingou, multiple upper quantiles are missed, depending on the model applied. Despite these discrepancies, the Q-Q plots generally indicate a good overall quantile fit across stations. These results suggest that the selected GEV models are reasonably effective in modelling maximum daily precipitation across the study area. Maximum daily rainfall series from stations with no significant trends are well fitted by the stationary GEV distribution, whereas series with significant trends are well fitted by non-stationary distributions. This implies that it is necessary to assess the trends in the series in order to make a judicious choice of the type of distribution (stationary or non-stationary).

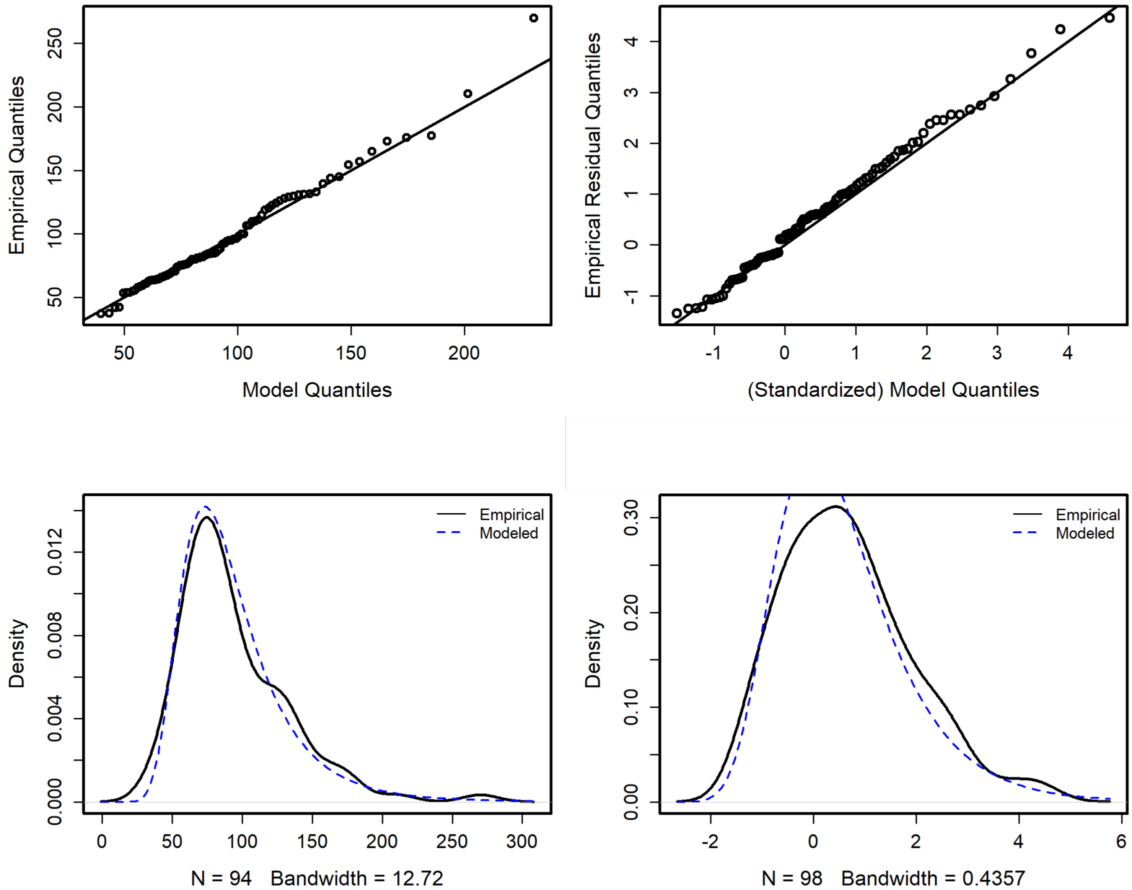

Figure 2. Goodness of fit of selected models at Grand Popo and Savè.

3.3. Precipitation Quantiles Evolution and Return Period of Maximum Recorded Precipitation

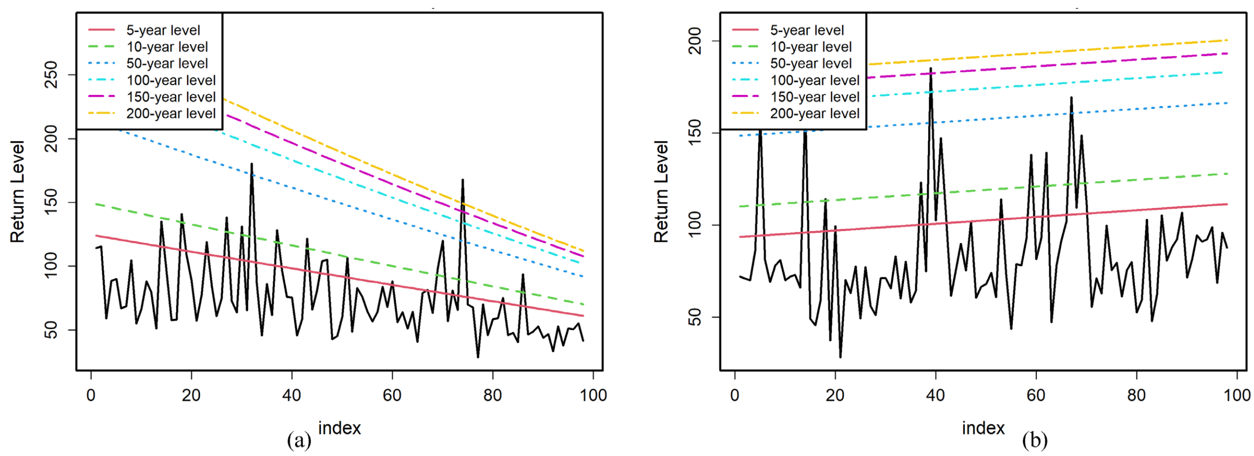

Figure 3. Evolution of return level with the non-stationary GEV model (a) Allada; (b) Adjohoun.

The temporal evolution of precipitation quantiles corresponding to various return periods using non-stationary GEV models (**Figure 3**) was analysed. Results indicate an increasing trend in the quantiles of maximum daily rainfall at Adjohoun (**Figure 3**), Sakété, and Abomey stations, suggesting a heightened frequency of extreme events over time. In contrast, a decreasing trend was observed at Allada (**Figure 3**), Cotonou, and Savè stations. However, the station of Adjohoun stands out, exhibiting an upward trend in annual rainfall quantiles. To assess the exposure of each station to extreme rainfall events, we compared the maximum daily rainfall records at each station with the rainfall amounts associated with return periods of 50, 100, 150, and 200 years. Our analysis revealed that Pobè, Sakété, Grand-Popo, and Kandi stations recorded at least one extreme daily rainfall event that exceeded the 200-year return period threshold. At Pobè, for example, the maximum daily rainfall was 192 mm, recorded in 1939, surpassing the estimated 200-year return level of 178 mm. Similarly, Sakété recorded 162.5 mm in 1954, exceeding its 200-year return period threshold of 154.2 mm. At Grand-Popo and Kandi, the highest recorded daily rainfall values were 270 mm in 1926 and 157.8 mm in 1964, respectively, both slightly above their respective 200-year return levels of 264 mm and 157 mm. For other stations, such as Adjohoun, Bopa, Cotonou, Parakou, and Porto-Novo, the recorded maximum daily rainfall amounts did not reach the 200-year return period threshold but did exceed or approach the 150-year return levels. Notable examples include 198.3 mm recorded at Adjohoun in 1960 and 208 mm at Porto-Novo in 1988, both values falling between the 150-year and 200-year return period levels. Stations such as Natitingou, Ouidah, and Zagnanado showed maximum daily rainfall values corresponding approximately to a 100-year return period. Additionally, in stations like Savè and Allada, where a declining trend in maximum daily rainfall has been observed, the highest rainfall events do not necessarily correspond to the highest return period events. For instance, the precipitation amount of 167.9 mm recorded at Allada in 1995 exceeds the 200-year return level, whereas 180.4 mm recorded in 1953 is associated with a return period of only 100 years. Overall, rainfall stations located in southern Benin (e.g., Allada, Pobè, Sakété, Grand-Popo, Adjohoun, Bopa, and Cotonou) exhibited higher extreme rainfall quantiles compared to those in the north (e.g., Parakou, Kandi, and Natitingou). Furthermore, these extreme rainfall events were predominantly concentrated during the period between 1922 and 1970, which corresponds to the historically wettest phase in the West African sub-region.

3.4. Discussion

The variability and breakpoints in the series of maximum daily rainfall were analyzed in this study. The data cover the period from 1921 to 2020, providing a century of observations. The results depended on the different methods used (Pettitt, Buishand, and Cross Entropy) to identify breakpoints. However, the results obtained using the Pettitt test are, in most cases, similar to those of the Buishand test. Generally, two key break periods were identified: one around the 1940s for some rainfall stations and around the 1960s for other stations. In a comparative analysis with other studies (Bessan et al., 2024; Babah-Daouda et al., 2021; Yabi & Afouda, 2012) which localized the breakpoint between 1969 and 1971, it is clear that the length of the data plays a crucial role in detecting breakpoints and analyzing trends. However, the detection of breakpoints can vary depending on the method used. For instance, the Pettitt and Buishand tests detected breakpoints in 1942 at Kandi and 1969 at Natitingou, while the Cross Entropy method identified breaks in 1957 and 1961, respectively. The different breakpoint dates detected in our study generally align with those identified by Lawin et al. (2019) in Benin. As highlighted by Servain et al. (2014), the use of long time series allows for a better capture of long-term climate variability and helps identify changes that could be masked in shorter series. Similar studies in Benin, such as Hountondji et al. (2011), have also shown that the detection of breakpoints can vary depending on the analysis period and the statistical method used. For instance, Babah-Daouda et al. (2021) identified breakpoints in 1989 and 1992 at the Tanguiéta and Djougou stations, respectively, for the period 1971-2020. Similarly, Ahokpossi (2018), a study covering the period 1940-2015, highlighted breakpoints in 1969 and 1990 at the Kandi and Cotonou stations. This contrasts with our study, which finds breakpoints around the 1960s and 1980s, if we only consider the period after 1950. This suggests that the earliest breakpoints can only be detected when the analysis period is long enough.

The breakpoints observed around the 1940s could be associated with broader climatic oscillations, particularly changes in the Pacific Decadal Oscillation (PDO), the Atlantic Multidecadal Oscillation (AMO), or Sea Surface Temperature (SST) anomalies that influence the West African Monsoon (Knight et al., 2005; Mohino et al., 2011). These ocean-atmosphere interactions likely influenced the observed changes in precipitation patterns and could reflect a phase shift toward a drier period preceding the major Sahelian droughts of the 1970s.

Furthermore, our results show spatial coherence in the break dates, particularly for coastal stations, with breakpoints mainly around 1969-1971. This spatial coherence is also documented by Akponikpè et al. (2019), who observed similar climate change patterns in the agro-ecological zones of Benin. Therefore, the use of different tests (Pettitt, Buishand, Cross Entropy) strengthens the robustness of our findings. Several studies have identified common breakpoints in both annual and maximum rainfall series. For example, Ahokpossi (2018) reported breakpoints in 1969 and 1990 for maximum and annual rainfall from 1940 to 2015, which correspond to some of our detections (in Natitingou and Parakou in 1969). Similarly, the 1969 breakpoint at Natitingou and the 1968 breakpoint at Bopa in our analysis align with findings from other studies (Bessan et al., 2024), reinforcing the hypothesis of significant climate change at these dates. These results are consistent with the studies by Aguilar et al. (2005) and Ozer et al. (2003), who also identified breakpoints in the 1960s and 1970s in West Africa, associated with the major Sahelian drought. These breakpoints may thus reflect regional climate changes rather than local variations.

The analysis of trends by sub-periods that we conducted is crucial for several reasons: it highlights changes in behavior before and after breakpoints, as shown by our results at Natitingou; it avoids biases associated with trend analysis over the entire period, which could mask significant variations, as noted by Descroix et al. (2020). The significant upward trends observed at Cotonou and Porto Novo from 1921-1970 are particularly noteworthy. These results differ from those of Kodja (2018), who identified mainly downward trends from 1951-2010. The trends observed in this study show significant variations compared to earlier research. For example, while some studies indicate a general downward trend in precipitation in Benin, this analysis reveals periods of significant increase, particularly at Cotonou and Porto Novo before 1970. This underscores the importance of segmenting data into sub-periods after identifying breakpoints.

The frequency analysis of maximum daily rainfall confirms that trend patterns are not uniform in the country. The stationary GEV distribution provides the best fit for some stations, while non-stationary GEV models are more appropriate for others. Stations such as Pobè, Zagnanado, Kandi, Parakou, Grand-Popo, Ouidah, and Bopa, which exhibit no significant trends over the 1921-2020 period, are best modelled using the stationary GEV distribution. Conversely, stations showing significant upward or downward trends, such as Savè and Cotonou, are more accurately represented by non-stationary GEV models. These findings are consistent with the results of Razi Ghalavand et al. (2025). The spatial difference in the trends and non-stationarity of extreme rainfall is affected by local-scale spatial factors such as latitude, longitude, elevation, slope direction, and gradient (Razi Ghalavand et al., 2025).

Non-stationary GEV models assume that one or more distribution parameters vary with time, implying that non-stationarity arises from temporal changes in the mean and/or variance of the rainfall series. Non-stationary GEV distribution with a decreasing trend (case of Savè and Allada) alters the intensity of the maximum of daily rainfall, while non-stationary GEV distribution with an increasing trend (case of Abomey and Adjohoun stations) intensifies the amount of the maximum of daily rainfall. This finding is consistent with Theng Hue et al. (2022), who reported similar behavior in potential evapotranspiration trends in Peninsular Malaysia. Specifically, for stations modelled with the GEV1 distribution, non-stationarity is attributed primarily to changes in the mean. In contrast, stations fitted with the GEV2 or GEV3 distributions exhibit changes in both mean and variance, reflecting more complex forms of non-stationarity.

Despite the methodological approach employed and the century-long dataset analyzed, this study has methodological limitations and inherent uncertainties associated with the analysis of very long-term rainfall time series in West Africa. Indeed, the study is constrained by the uneven spatial distribution of rainfall stations across Benin. There is a higher concentration of stations in the southern and coastal regions compared to the north. This spatial disparity may introduce bias in the regional representativeness of trends and breakpoints, particularly in characterizing rainfall extremes in the less-instrumented northern areas. In addition, due to the temporal heterogeneity of missing data and station-specific issues, errors may occur during data processing. Examples include temporal gaps in the records and changes in measurement techniques over time (e.g., from manual observations by agents to automated instruments). Such factors are likely to introduce significant uncertainties in both trend estimation and the accurate detection of breakpoints. The exclusive use of annual maximum daily rainfall (Annual Maximum Series), although a standard practice in extreme hydrology, represents a major limitation, as it does not capture the evolution of short-duration, high-intensity rainfall events (sub-daily extremes). To overcome these limitations, future research should consider integrating reanalysis datasets or outputs from high-resolution Regional Climate Models (RCMs). These approaches could enable cross-validation of the spatial coherence of detected trends and improve the analysis of rainfall extremes at finer temporal scales, thereby strengthening the robustness of the conclusions.

4. Conclusion

In this study, trends and frequency analysis of the maximum annual daily rainfall series were assessed for rainfall stations with a 100-year history. The trends observed in this study show significant variations compared to earlier research. The analysis of trends by sub-periods that we conducted is crucial for several reasons: it highlights changes in behavior before and after breakpoints, as shown by our results in Natitingou; it avoids biases associated with trend analysis over the entire period, which could mask significant variations. For example, while some studies indicate a general downward trend in precipitation in Benin, this analysis reveals periods of significant increase, particularly in Cotonou and Porto Novo before

1970. This underscores the importance of segmenting data into sub-periods after identifying breakpoints. The frequency analysis indicates that the stationary GEV distribution adequately fits rainfall time series without significant trends, whereas non-stationary GEV models are more suitable for time series exhibiting significant trends. These findings suggest that the observed non-stationarity and trends in extreme rainfall are primarily driven by changes in the mean and/or variance of the series.

Conflicts of Interest

The authors declare no conflicts of interest regarding the publication of this paper.

References

Aguilar, E. T., Peterson, C., Ramírez Obando, P., Frutos, R., Retana, J. A. et al. (2005). Changes in Precipitation and Temperature Extremes in Central America and Northern South America, 1961-2003. *Journal of Geophysical Research: Atmospheres, 110,* D23107. https://doi.org/10.1029/2005jd006119

Ahokpossi, Y. (2018). Analysis of the Rainfall Variability and Change in the Republic of Benin (West Africa). *Hydrological Sciences Journal, 63,* 2097-2123. https://doi.org/10.1080/02626667.2018.1554286

Akponikpè, P. B. I., Tovihoudji, P., Lokonon, B., Kpadonou, E. et al. (2019). *Etude de Vulnérabilité aux changements climatiques du Secteur Agriculture au Bénin. Report Produced under the Project "Projet d'Appui Scientifique aux processus de Plans Nationaux d'Adaptation dans les pays francophones les moins avancés d'Afrique subsaharienne".* Climate Analytics gGmbH.

Ampofo, S., Annor, T., Aryee, J. N. A., Atiah, W. A., & Amekudzi, L. K. (2023). Long-Term Spatio-Temporal Variability and Change in Rainfall over Ghana (1960-2015). *Scientific African, 19,* e01588. https://doi.org/10.1016/j.sciaf.2023.e01588

Babah-Daouda, M., Yabi, A. J., & Orou Wari, B. (2021). Variabilité climatique et rendement maraicher dans les communes de Djougou et de Tanguiéta au Nord-Bénin. *International Journal of Biological and Chemical Sciences, 15,* 1923-1936. https://doi.org/10.4314/ijbcs.v15i5.19

Bera, S. (2017). Trend Analysis of Rainfall in Ganga Basin, India during 1901-2000. *American Journal of Climate Change, 6,* 116-131. https://doi.org/10.4236/ajcc.2017.61007

Bessan, V. M., Vissin, W. E., Ogou, K. F., & Ogouwale, E. (2024). Variabilité des précipitations pour la période 1960-2022 dans le département du Mono, République du Bénin, Afrique de l'Ouest. *Afrique Science Revue Internationale des Sciences et Technologie, 25,* 37-50.

Buishand, T. A. (1982). Some Methods for Testing the Homogeneity of Rainfall Records. *Journal of Hydrology, 58,* 11-27. https://doi.org/10.1016/0022-1694(82)90066-x

Buishand, T. A. (1984). Tests for Detecting a Shift in the Mean of Hydrological Time Series. *Journal of Hydrology, 73,* 51-69. https://doi.org/10.1016/0022-1694(84)90032-5

Chikobvu, D., & Chifurira, R. (2015). Modelling of Extreme Minimum Rainfall Using Generalised Extreme Value Distribution for Zimbabwe. *South African Journal of Science, 111,* 1-8. https://doi.org/10.17159/sajs.2015/20140271

Claeskens, G., & Hjort, N. (2008). *Model Selection and Model Averaging.* Cambridge University Press.

Coles, S. (2001). *An Introduction to Statistical Modeling of Extreme Values.* Springer.

Descroix, L., Sané, Y., Thior, M., Manga, S., Ba, B. D., Mingou, J. et al. (2020). Inverse Estuaries in West Africa: Evidence of the Rainfall Recovery? *Water, 12,* Article 647. https://doi.org/10.3390/w12030647

Donat, M. G., Lowry, A. L., Alexander, L. V., O'Gorman, P. A., & Maher, N. (2016). More Extreme Precipitation in the World's Dry and Wet Regions. *Nature Climate Change, 6,* 508-513. https://doi.org/10.1038/nclimate2941

El Kasri, J., Lahmili, A., Soussi, H., Jaouda, I., & Bentaher, M. (2021). Trend Analysis of Meteorological Variables: Rainfall and Temperature. *Civil Engineering Journal, 7,* 1868-1879. https://doi.org/10.28991/cej-2021-03091765

Gao, T., Wang, H. J., & Zhou, T. (2017). Changes of Extreme Precipitation and Nonlinear Influence of Climate Variables over Monsoon Region in China. *Atmospheric Research, 197,* 379-389. https://doi.org/10.1016/j.atmosres.2017.07.017

Gardner, L. A. (1969). On Detecting Changes in the Mean of Normal Variates. *The Annals of Mathematical Statistics, 40,* 116-126. https://doi.org/10.1214/aoms/1177697808

Hajani, E. (2022). The Influence of Climate Change and Variability on the IFD Curves in NSW, Australia. *Science of the Total Environment, 845,* Article 157359. https://doi.org/10.1016/j.scitotenv.2022.157359

Hountondji, Y. C., de Longueville, F., & Ozer, P. (2011). Trends in Extreme Rainfall Events in Benin (West Africa), 1961-2000. In *Proceedings of the 1st International Conference on Energy, Environment and Climate Change* (pp. 7). http://hdl.handle.net/2268/96112 https://www.academia.edu/2480974

IPCC (2007). Climate Change, 2007: The Scientific Basis. In *Contribution of Working Group I to the Fourth Assessment Report of the Intergovernmental Panel on Climate Change* (p. 996). Cambridge University Press.

IPCC (2021). Climate Change 2021: The Physical Science Basis. In *Contribution of Working Group I to the Sixth Assessment Report of the Intergovernmental Panel on Climate Change* (p. 2391). Cambridge University Press.

Jaagus, J. (2006). Trends in Sea Ice Conditions in the Baltic Sea near the Estonia, Coast during the Period 1949/1950–2003/2004 and Their Relationships to Large Scale Atmospheric Circulation. *Boreal Environment Research, 11,* 169-183.

Jayaweera, L., Wasko, C., & Nathan, R. (2024). Modelling Non-Stationarity in Extreme Rainfall Using Large-Scale Climate Drivers. *Journal of Hydrology, 636,* Article 131309. https://doi.org/10.1016/j.jhydrol.2024.131309

Jayaweera, L., Wasko, C., & Nathan, R. (2025). Evidence for Non-Stationarity in the GEV Shape Parameter When Modeling Extreme Rainfall. *Water Resources Research, 61,* e2023WR036426. https://doi.org/10.1029/2023wr036426

Kang, H. M., & Yusof, F. (2010). *Homogeneity Tests on the Daily Rainfall Series in Peninsular Malaysia*. https://api.semanticscholar.org/CorpusID:128038360

Katz, R. W., Parlange, M. B., & Naveau, P. (2002). Statistics of Extremes in Hydrology. *Advances in Water Resources, 25,* 1287-1304. https://doi.org/10.1016/s0309-1708(02)00056-8

Kendall, M. (1975). *Rank Correlation Techniques*. Charles Griffen.

Khaliq, M. N., & Ouarda, T. B. M. J. (2006). On the Critical Values of the Standard Normal Homogeneity Test (SNHT). *International Journal of Climatology, 27,* 681-687. https://doi.org/10.1002/joc.1438

Knight, J. R., Allan, R. J., Folland, C. K., Vellinga, M., & Mann, M. E. (2005). A Signature of Persistent Natural Thermohaline Circulation Cycles in Observed Climate. *Geophysical Research Letters, 32,* 1-4. https://doi.org/10.1029/2005gl024233

Kodja, D. J. (2018). *Indicateurs des évènements hydroclimatiques extrêmes dans le bassin versant de l'Ouémé à l'exutoire de Bonou en Afrique de l'Ouest.* Thèse de Géographie, Université Montpellier.

Kougbeagbede, H., Hounvou S. F., Houeto A., & Waidi O. (2024). Analysis of Extreme Daily Rainfall in Cotonou, Benin (West Africa). *International Journal of Environment and Climate Change, 14,* 666-673.

Kpanou, M., Laux, P., Brou, T., Vissin, E., Camberlin, P., & Roucou, P. (2021). Spatial Patterns and Trends of Extreme Rainfall over the Southern Coastal Belt of West Africa. *Theoretical and Applied Climatology, 143,* 473-487. https://doi.org/10.1007/s00704-020-03441-8

Kumar, U., Singh, D. K., Panday, S. C., Bisht, J. K., & Kant, L. (2023). Spatio-temporal Trend and Change Detection of Rainfall for Kosi River Basin, Uttarakhand Using Long-Term (115 Years) Gridded Data. *Arabian Journal of Geosciences, 16,* Article No. 173. https://doi.org/10.1007/s12517-023-11244-0

Kuniyal, J. C., Kanwar, N., Bhoj, A. S., Rautela, K. S., Joshi, P., Kumar, K. et al. (2021). Climate Change Impacts on Glacier-Fed and Non-Glacier-Fed Ecosystems of the Indian Himalayan Region: People's Perception and Adaptive Strategies. *Current Science, 120,* 888-899. https://doi.org/10.18520/cs/v120/i5/888-899

Lawin, A. E., Hounguè, N. R., Biaou, C. A., & Badou, D. F. (2019). Statistical Analysis of Recent and Future Rainfall and Temperature Variability in the Mono River Watershed (Benin, Togo). *Climate, 7,* Article 8. https://doi.org/10.3390/cli7010008

Mann, H. B. (1945). Nonparametric Tests against Trend. *Econometrica, 13,* Article 245. https://doi.org/10.2307/1907187

Martins, E. S., & Stedinger, J. R. (2001). Historical Information in a Generalized Maximum Likelihood Framework with Partial Duration and Annual Maximum Series. *Water Resources Research, 37,* 2559-2567. https://doi.org/10.1029/2000wr000009

Mei, C., Liu, J., Chen, M., Wang, H., Li, M., & Yu, Y. (2018). Multi-Decadal Spatial and Temporal Changes of Extreme Precipitation Patterns in Northern China (Jing-Jin-Ji District, 1960–2013). *Quaternary International, 476,* 1-13. https://doi.org/10.1016/j.quaint.2018.03.008

Mohino, E., Janicot, S., & Bader, J. (2011). Sahel Rainfall and Decadal to Multi-Decadal Sea Surface Temperature Variability. *Climate Dynamics, 37,* 419-440. https://doi.org/10.1007/s00382-010-0867-2

Morio, J., Pastel, R., & Le Gland, F. (2011). Estimation de probabilités et de quantiles rares pour la caractérisation d'une zone de retombée d'un engin. *Journal de la société française de statistique, 152,* 1-29. http://www.numdam.org/item/JSFS_2011__152_4_1_0/

Obada, E., Alamou, E. A., Biao, E. I., & Zandagba, E. B. J. (2021). Interannual Variability and Trends of Extreme Rainfall Indices over Benin. *Climate, 9,* Article 160. https://doi.org/10.3390/cli9110160

Obada, E., Alamou, E., Chabi, A., Zandagba, J., & Afouda, A. (2017). Trends and Changes in Recent and Future Penman-Monteith Potential Evapotranspiration in Benin (West Africa). *Hydrology, 4,* Article 38. https://doi.org/10.3390/hydrology4030038

Ozer, P., Erpicum, M., Demarée, G., & Vandiepenbeeck, M. (2003). The Sahelian Drought May Have Ended during the 1990s. *Hydrological Sciences Journal, 48,* 489-492. https://doi.org/10.1623/hysj.48.3.489.45285

Pettitt, A. N. (1979). A Non-Parametric Approach to the Change-Point Problem. *Applied Statistics, 28,* 126-135. https://doi.org/10.2307/2346729

Programme Alimentaire Mondial des Nations Unies (PAM) (2014). *Analyse Globale de la*

Vulnérabilité et de la Sécurité Alimentaire (AGVSA) en République du Bénin. https://documents.wfp.org/stellent/groups/public/documents/ena/wfp203247.pdf

Prosdocimi, I., & Kjeldsen, T. (2021). Parametrisation of Change-Permitting Extreme Value Models and Its Impact on the Description of Change. *Stochastic Environmental Research and Risk Assessment, 35,* 307-324. https://doi.org/10.1007/s00477-020-01940-8

Razi Ghalavand, M., Farajzadeh, M., & Ghavidel Rahimi, Y. (2025). Modeling Return Levels of Non-Stationary Rainfall Extremes Due to Climate Change. *Atmosphere, 16,* Article 136. https://doi.org/10.3390/atmos16020136

Rubinstein, R., & Kroese, D. (2004). *The Cross-Entropy Method: A Unified Approach to Combinatorial Optimization, Monte-Carlo Simulation, and Machine-Learning*. Springer-Verlag.

Sen, P. (1968). Estimates of the Regression Coefficient Based on Kendall's Tau. *Journal of the American Statistical Association, 63,* 1379-1389. https://doi.org/10.1080/01621459.1968.10480934

Servain, J., Caniaux, G., Kouadio, Y. K., McPhaden, M. J., & Araujo, M. (2014). Recent Climatic Trends in the Tropical Atlantic. *Climate Dynamics, 43,* 3071-3089. https://doi.org/10.1007/s00382-014-2168-7

Tabari, H., & Talaee, P. H. (2011). Temporal Variability of Precipitation over Iran: 1966–2005. *Journal of Hydrology, 396,* 313-320. https://doi.org/10.1016/j.jhydrol.2010.11.034

Theng Hue, H., Ng, J. L., Huang, Y. F., & Tan, Y. X. (2022). Evaluation of Temporal Variability and Stationarity of Potential Evapotranspiration in Peninsular Malaysia. *Water Supply, 22,* 1360-1374. https://doi.org/10.2166/ws.2021.343

Wijngaard, J. B., Klein Tank, A. M. G., & Können, G. P. (2003). Homogeneity of 20th Century European Daily Temperature and Precipitation Series. *International Journal of Climatology, 23,* 679-692. https://doi.org/10.1002/joc.906

World Bank (2011). *Benin-Inondations au Bénin: Rapport d'Evaluation des Besoins Post-Catastrophe*. World Bank Group. http://documents.worldbank.org/curated/en/750141468208769683/Benin-Inondations-au-Benin-rapportdevaluation-des-besoins-post-catastrophe

Wu, Y., & Polvani, L. M. (2017). Recent Trends in Extreme Precipitation and Temperature over Southeastern South America: The Dominant Role of Stratospheric Ozone Depletion in the CESM Large Ensemble. *Journal of Climate, 30,* 6433-6441. https://doi.org/10.1175/jcli-d-17-0124.1

Yabi, I., & Afouda, F. (2012). Extreme Rainfall Years in Benin (West Africa). *Quaternary International, 262,* 39-43. https://doi.org/10.1016/j.quaint.2010.12.010

Yang, Y., Weng, B., Man, Z., Yu, Z., & Zhao, J. (2020). Analyzing the Contributions of Climate Change and Human Activities on Runoff in the Northeast Tibet Plateau. *Journal of Hydrology: Regional Studies, 27,* Article 100639. https://doi.org/10.1016/j.ejrh.2019.100639